Structural Characterization and Pharmacology of a Potent (Cys101–Cys119, Cys110–Cys117) Bicyclic Agouti-Related Protein (AGRP) Melanocortin Receptor Antagonist

Andrzej Wilczynski,[†,‡] Xiang S. Wang,[‡,§] Rayna M. Bauzo,[†] Zhimin Xiang,[†] Amanda M. Shaw,[ǁ] William J. Millard,[ǁ] Nigel G. Richards,[§] Arthur S. Edison,[⊥] and Carrie Haskell-Luevano*,[†]

Departments of Medicinal Chemistry, Chemistry, Pharmacodynamics, and Biochemistry and Molecular Biology, University of Florida, Gainesville, Florida 32610

Agouti-related protein (AGRP) is one of two known naturally occurring antagonists of G-protein coupled receptors. AGRP is synthesized in the brain and is an antagonist of the melanocortin-3 and -4 receptors (MC3R, MC4R). These three proteins are involved in the regulation of energy homeostasis and obesity in both mice and humans. The human AGRP protein is 132 amino acids and contains five disulfide bridges in the C-terminal domain. Previous reports of the NMR structures of hAGRP(87–132) and a truncated 34 amino acid form consisting of four disulfide bridges identified that AGRP contains an inhibitor cystine knot (ICK) structural fold, and that is the first mammalian example. Herein, we report a bicyclic hAGRP analogue that, when compared to hAGRP(87–132), possesses equal binding affinity but is 80-fold less potent at the mouse MC4R. Using NMR, computer assisted molecular modeling (CAMM), and cluster analysis, we have identified five structural families, two of which are highly populated, of this bicyclic hAGRP analogue. Computational docking experiments of this bicyclic hAGRP derivative, using a three-dimensional homology molecular model of the mouse MC4R, identified that three of the five structural families could be docked into the MC4R without problems from steric hindrance. Those three docked mMC4R-bicyclic hAGRP family structures were compared with putative hAGRP(87–132) ligand–receptor interactions previously reported (Wilczynski et al. *J. Med. Chem.* **2004**, *47*, 2194) in attempts to identify a "bioactive" conformation of the bicyclic hAGRP peptide and account for the 80-fold decreased ligand potency compared to hAGRP(87–132).

Introduction

Agouti-related protein (AGRP) is one of two known endogenous antagonists of G-protein coupled receptors (GPCRs) identified to date and specifically antagonizes the melanocortin receptors expressed in the brain, the melanocortin-3 and -4 receptors (MC3R, MC4R).[1] Both the AGRP and the MC4R proteins have been determined to physiologically regulate food intake and participate in obesity and energy homeostasis.[1,2] Additionally, AGRP may function in vivo as an inverse agonist (decrease basal cAMP levels in the absence of agonist ligand) at the MC4R.[3–5] AGRP may be an important therapeutic target for both the understanding and treatment of obesity related diseases and the involvement of the melanocortin system in the neuroendocrine regulation of energy homeostasis. Surprisingly, very little is currently known about specific molecular interactions of AGRP with the melanocortin receptors, the mechanism(s) regulating food intake and obesity, and the molecular interactions with the auxiliary protein families (mahogany/attractin and syndecans) that are postulated to interact with AGRP upstream of the MC4R.[6–9]

The C-terminal domain of the hAGRP peptide has been identified as possessing nearly equipotent melanocortin receptor pharmacology as the full length endogenous form of this hormone.[1,10] Structural reports by Millhauser et al. of hAGRP(87–132) and "mini-AGRP" identified a unique mammalian inhibitor cystine knot (ICK) fold involving the three hAGRP (Cys87–Cys102, Cys94–Cys108, and Cys101–Cys119) disulfide bridges that is important for the structure and orientation of the hAGRP active loop 110–117 amino acids.[11,12] It has also been identified that the core monocyclic decapeptide hAGRP(109–118) possesses μM antagonism at the central MC3 and MC4 receptors, and agonist activity at the peripheral MC1R.[13,14] Furthermore, monocyclic hAGRP peptides of varying length resulted in high nM to μM pharmacology at the melanocortin receptors.[15] On the basis of these cumulative data, previous presentations of bicyclic derivatives,[16] and the "mini-AGRP" design, structure, and pharmacology,[12,17] we hypothesized that there must be additional structural information outside the monocyclic hAGRP templates we have utilized previously that can be identified and used for drug design purposes.[14,15,18] In attempts to identify a sequence of minimal length and minimal side chain cyclizations, yet still maintain nM mMC4R pharmacol-

* To whom correspondence should be addressed: University of Florida, Department of Medicinal Chemistry, PO Box 100485, Gainesville, FL 32610. Tel: (352) 846-2722. Fax: (352) 392-8182. E-mail: Carrie@cop.ufl.edu.
† Department of Medicinal Chemistry.
‡ These authors contributed equally to this manuscript.
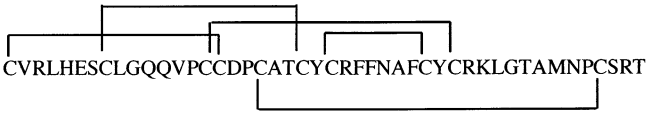§ Department of Chemistry.
ǁ Department of Pharmacodynamics.
⊥ Department of Biochemistry and Molecular Biology.

Table 1. Analytical Data for the Peptides Synthesized in This Study

Peptide	Structure	HPLC k' (system 1)[a]	HPLC k' (system 2)[a]	Purity (%)	Observed molecular mass	Calculated molecular mass
1	CUDPUATUYCRFFNAFCYCRKL	7.1	12.1	>98	2572.9	2573.1
2	HESCLGQQVPCUDPUATCYURFFNAFUYCRKL	6.2	11.3	>98	3635.4	3634.2

[a] HPLC k' = [(peptide retention time − solvent retention time)/solvent retention time] in solvent system 1 (10% acetonitrile in 0.1% trifluroacetic acid/water and a gradient to 90% acetonitrile over 35 min) or solvent system 2 (10% methanol in 0.1% trifluroacetic acid/water and a gradient to 90% methanol over 35 min). An analytical Vydac C_{18} column (Vydac 218TP104) was used with a flow rate of 1.5 mL/min. The percentage peptide purity is determined by HPLC at a wavelength of 214 λ.

Table 2. Pharmacology of the AGRP Based Ligands at the Mouse Melanocortin Receptors[a]

| Peptide	Structure	mMC1R Agonist EC_{50} (nM)	mMC3R Antagonist pA_2 IC_{50} (nM)	mMC4R Antagonist pA_2 IC_{50} (nM)
hAGRP(87-132)	CVRLHESCLGQQVPCCDPCATCYCRFFNAFCYCRKLGTAMNPCSRT	>100,000	pA_2=8.9±0.2 IC_{50}=2.8±0.4	pA_2=9.4±1.0 IC_{50}=3.0±0.3
Mini-hAGRP	Ac-CVRLHESCLGQQVPCCDPAATCYCRFFNAFCYCR-NH$_2$	>100,000	pA_2=8.1±0.1 IC_{50}=4.8±1.2	pA_2=8.5±0.1 IC_{50}=1.0±0.6
hAGRP(109-118)*	YCRFFNAFCY-NH$_2$	5,120±3,040	>100,000 IC_{50}=11700 ±3900*	pA_2=6.8±0.24 IC_{50}=275±60*
1	CUDPUATUYCRFFNAFCYCRKL	1,460±720	pA_2=6.8±0.3 IC_{50}=140±33	pA_2=7.5±0.2 IC_{50}=10±4
2	HESCLGQQVPCUDPUATCYURFFNAFUYCRKL	>100,000	pA_2=5.6±0.6 40%	pA_2=6.3±0.2 IC_{50}=880±390

[a] The indicated errors for the functional data (pA_2 or EC_{50}) represent the standard error of the mean determined from at least three independent experiments, whereas the indicated errors in the binding assay (IC_{50}) represent the standard deviation determined from two independent experiments. The antagonistic pA_2 values were determined using the Schild analysis and the agonist MTII. $K_i = -\log pA_2$. >100,000 indicates that the compound was examined but lacked agonist or antagonist properties at up to 100 μM concentrations. The binding IC_{50} values were obtained by using the I^{125}-hAGRP(87−132) radiolabel to competitively displace the ligand. The percentage listed represents the percent specific binding of the I^{125}-hAGRP(87−132) radiolabel displaced by the ligand at 10 μM concentrations. (*) The values indicated for the hAGRP(109−118) peptide have been previously reported in ref 14, and the IC_{50} values were determined using I^{125}-MTII. The U amino acid abbreviation represents amino butyric acid.

ogy, we synthesized and pharmacologically characterized two bicyclic peptides based upon the hAGRP template. These peptides were selected on the basis of the selection of retaining two endogenous disulfide bridges, extending the sequence beyond the central "loop" domain, and replacing the endogenous Cys residues not used for cyclization with the pseudo isostere α-aminobutyric acid (Abu, U). Additionally, both the Cys to Abu substitution and the choice of bicyclic peptides had been previously presented by Amgen to result in potentially interesting compounds.[16]

Results

Melanocortin Receptor Pharmacology. The bicyclic hAGRP based peptides reported in this study were synthesized using standard Fmoc solid-phase peptide synthesis, analytically verified (Table 1), and pharmacologically characterized at the mouse melanocortin receptor isoforms MC1R and MC3−5R. The ability of the bicyclic ligands to competitively displace I^{125}-hAGRP(87−132) in a dose−response manner was evaluated at the MC3 and MC4 receptors (Table 2, Figure 1). The MC3R and MC4R were the only melanocortin receptor isoforms used for competitive displacement binding studies since hAGRP only functionally antagonizes these receptors[1] and not the MC1R or MC5R.[10] Intracellular cAMP based functional agonist and antagonist bioassays were performed for each bicyclic ligand at the mMC1R and mMC3−5R, Table 2 and Figures 2 and 3. At the mMC1R, peptide 1 possessed a full agonist dose−response in the μM EC_{50} range (Figure 3), whereas peptide 2 did not possess any mMC1R agonist activity at up to 100 μM concentrations (data not shown). Both peptides 1 and 2 lacked agonist or antagonist pharmacology at the mMC5R at up to 100 μM concentrations.
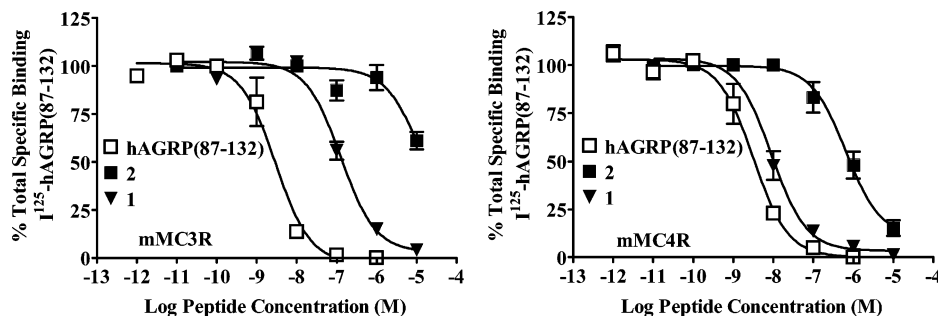
Figure 1. Comparison of hAGRP ligand binding at the mouse MC3 and MC4 receptors. Radiolabeled I^{125}-hAGRP(87−132) was utilized for these studies.
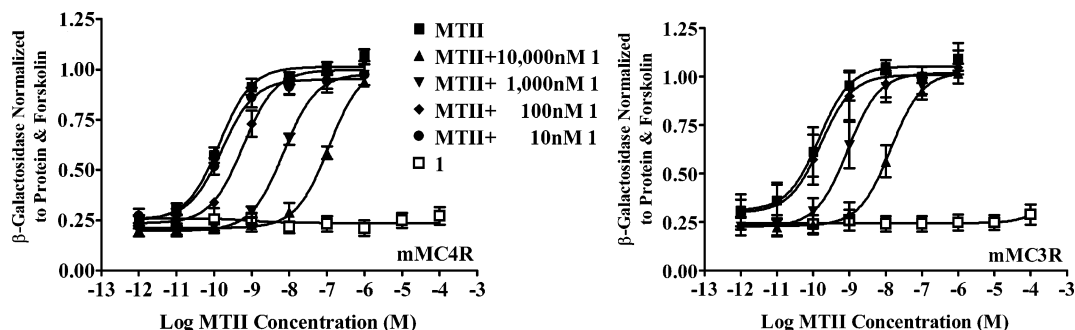
Figure 2. Antagonist pharmacology of peptide 1 at the mouse MC3 and MC4 receptors. A Schild antagonist experimental design was applied and the agonist MTII was utilized in these studies.
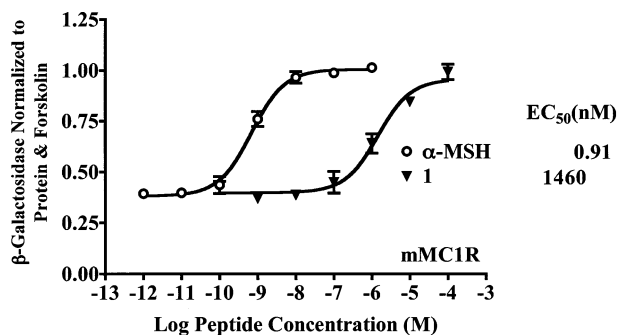
**Figure 3.** Agonist pharmacology of peptide 1, relative to the melanocortin agonist α-MSH at the mouse MC1 receptor.

At the mMC4R, peptide 1 possessed equipotent (within the inherent 3-fold experimental error due to standard weighing and pipetting associated limitations) binding affinity, but was an 80-fold less potent antagonist than hAGRP(87−132). This bicyclic peptide 1 hAGRP derivative is 22 amino acids in length and contains only two of the five endogenous disulfide bridges found in hAGRP, or four disulfide bridges in the mini-AGRP template (Table 2), but still results in equipotent binding affinity at the mMC4R as compared to both hAGRP(87−132) and mini-hAGRP, within experimental error. Presumably, the decrease in peptide 1 potency is due to a lack of "key" ligand−receptor interactions or a change in ligand desolvation energy. The bicyclic peptide 2 contains two disulfide bridges found in the native hAGRP structure, but it is lacking the disulfide bridge encompassing the core (hAGRP 110−117) Cys-Arg-Phe-Phe-Asn-Ala-Phe-Cys octapeptide domain (Table 2), previously believed to be critical for the functional activity of the hAGRP molecule.[13] Interestingly, this peptide still retains antagonist pharmacology at the central MC3 and MC4 receptors, albeit at high nM to μM efficacies. The 32 amino acid bicyclic peptide 2 was only able to competitively displace 40% of the radiolabeled I^{125}-hAGRP(87−132) at the mMC3R (Figure 1) at concentrations of 1 μM, which correlates with the functional antagonist pA_2 value of 5.6 (Table 2). Thus, presumably at increased concentrations, the bicyclic analogue **2** would be able to competitively displace the radiolabeled ligand at the mMC3R corresponding with the functional μM antagonist efficacy. At the mMC4R, peptide 2 possessed a high nM binding affinity and possessed ca. 300-fold decreased binding affinity, as compared with the hAGRP(87−132) and mini-hAGRP multicyclic peptides. Functionally, peptide 2 possessed 1250- to 2000-fold decreased antagonist potency at the mMC3 and mMC4 receptors, but was only ca. 15-fold less potent than peptide 1 at these respective melanocortin receptors. On the basis of the binding affinity and antagonist potency of the 22 amino acid bicyclic hAGRP peptide 1 analogue, we decided to perform NMR, computer assisted molecular modeling (CAMM), and receptor homology molecular modeling studies of this ligand.

NMR and CAMM Based Structures. Although peptide 1 is just 22 amino acids in length and somewhat constrained by the presence of two disulfide bridges, some regions of the NMR spectrum were extremely overlapped and challenging to assign. Specifically, the region from about 8.0 to 8.2 ppm was very crowded, but many of the other resonances were well-dispersed (Figure 4). This overlap also made some NOEs difficult to assign, and the assignment of one NOE (U_8H^α−$C_{10}H^N$) could only be determined following an initial RMD simulation. Table 3 lists the complete assignment of all residues in the peptide 1 bicyclic hAGRP analogue.

Proton distance values obtained from the NOESY NMR spectra, as described in the Experimental Section (Figure 5), were used for ligand structural studies using computer assisted molecular modeling (CAMM). The use of CAMM for a molecule like peptide 1, based upon
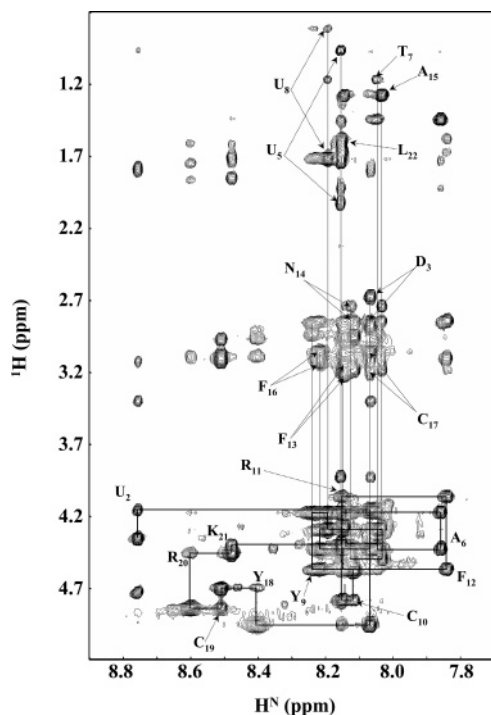
Figure 4. Expansion of the NOE experiment identifying the chemical shift assignments of peptide 1 amino acid residues. The one letter amino acid abbreviations are designated with U representing the α-amino butyric amino acid used to replace the Cys residues in corresponding positions in hAGRP(87−132).

Table 3. ^{1}H NMR Chemical Shift Values for Peptide 1 Dissolved in 95% H_2O/5% D_2O at 30 °C

amino acid position	H^N	H$^\alpha$	H$^\beta$	other
Cys1		4.35	3.39, 3.12	
Abu2^a	8.76	4.16	1.79	γ-0.96
Asp3	8.07	4.95	2.67, 2.88	
Pro4		4.42	2.33	γ-2.04, δ-3.92
Abu5	8.15	4.18	1.92	γ-0.95
Ala6	7.86	4.42	1.44	
Thr7	8.04	4.30	4.18	γ-1.17
Abu8^a	8.19	4.17	1.72	γ-0.82
Tyr9	8.24	4.57	2.86, 2.94	2,6H-7.05, 3,5H and/or 4H-6.77
Cys10	8.12	4.79	2.95, 3.19	
Arg11	8.15	4.06	1.67, 1.56	γ-1.45, 1.33, δ-3.06
Phe12	7.84	4.56	2.85, 3.10	2,6H-7.21, 3,5H and/or 4H-7.33
Phe13	8.14	4.44	3.14, 3.23	2,6H-7.23, 3,5H and/or 4H-7.34
Asn14	8.12	4.50	2.73, 2.84	NH$_2$-6.80, 7.45
Ala15	8.03	4.28	1.28	
Phe16	8.22	4.43	3.05, 3.14	2,6H-7.18
Cys17	8.07	4.95	3.05, 2.88	
Tyr18	8.40	4.69	2.97, 3.10	2,6H-7.10, 3,5H and/or 4H-6.78
Cys19	8.51	4.84	2.97, 3.10	
Arg20	8.60	4.46	1.86, 1.74	γ-1.60, δ-3.09
Lys21	8.48	4.39	1.84, 1.69	γ-1.41
Leu22	8.16	4.26	1.61	

^{a} Abu is α-aminobutyric acid.

NMR proton distance values, possesses an inherent risk of becoming "trapped" in local energy minima due to improper formation of disulfide bonds. Therefore, we performed extensive RMD simulations with unambiguous NMR distance restraints before we covalently formed the disulfide bonds. At the end of these initial simulations, the Cys amino acids that have been determined to participate in side chain cyclizations were found to be in the proper orientation to easily form the
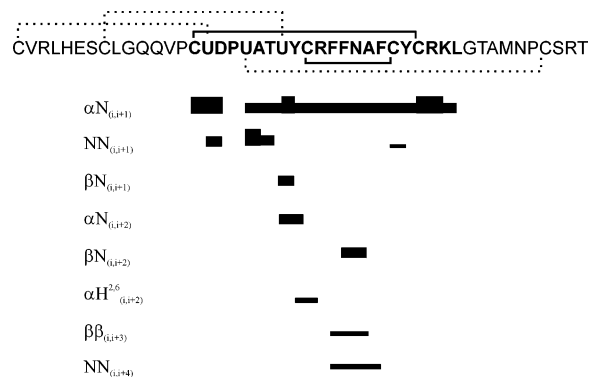

Figure 5. Summary of the NOE intensities observed for peptide 1. The additional amino acids outside peptide 1 residues (bold) represent the hAGRP(87−132) residues that are absent in peptide 1 for prospective and comparative purposes. The hashed disulfide bridges represent those found in hAGRP(87−132), but absent in AMW2−92. The height of the bar indicates the strength of the NOE.

two disulfides without significant distortions in the molecule. Following the initial formation of the disulfides, we first allowed the molecule to fully relax by energy minimization before doing a complete RMD simulation on the complete peptide 1 compound using all the experimentally identified NMR distance restraints.

Conformational families of structures were identified by energy minimizing 167 evenly spaced points along a 17 ns RMD trajectory. The CAMM structures of peptide 1 generated on the basis of the NMR structural data clearly had multiple conformations, since superposition of all the members did not result in a clear structure (data not shown). We therefore did a cluster analysis of the structures and grouped them by backbone (ϕ, ψ) dihedral angles.[18] This cluster analysis yielded five distinct subfamilies of structures, two of which were highly populated (Figure 6). Three of the subfamilies were very sparsely populated with less than 2% of the total number of total identified conformers. As illustrated in Figure 5, the major NMR restraints are primarily located in the octapeptide Cys-Arg-Phe-Phe-Asn-Ala-Phe-Cys (hAGRP 110−117) "active" region of peptide 1 involving the inner loop containing the Arg-Phe-Phe residues identified as "key" for hAGRP function. On the basis of these results, we focused on this region in the analysis that follows.

The hAGRP(110−117) active site loop residues Cys-Arg-Phe-Phe-Asn-Ala-Phe-Cys of each of the five representative structures of peptide 1 were superposed with the comparable residues from the high-resolution NMR structure of hAGRP(87−132) (PDB: 1HYK).[11] Although the (hAGRP 110−117) active site loop primary structure is nearly identical for peptide 1 and hAGRP(87−132), we observed several additional NOEs in the region of the Arg-Phe-Phe residues that were not reported in the hAGRP(87−132) analysis.[11] This is not entirely unexpected, because the peptide 1 not only is shorter than hAGRP(87−132) but also is lacking three disulfide bridges that may significantly influence the conformation of the active site hAGRP(110−117) residues. Despite the differences in NOE data, a superposition of the active site loop hAGRP(110−117) residues of AGRP (87−132) and the major conformational family of peptide 1 has a relatively low RMSD of 1.4 Å for backbone
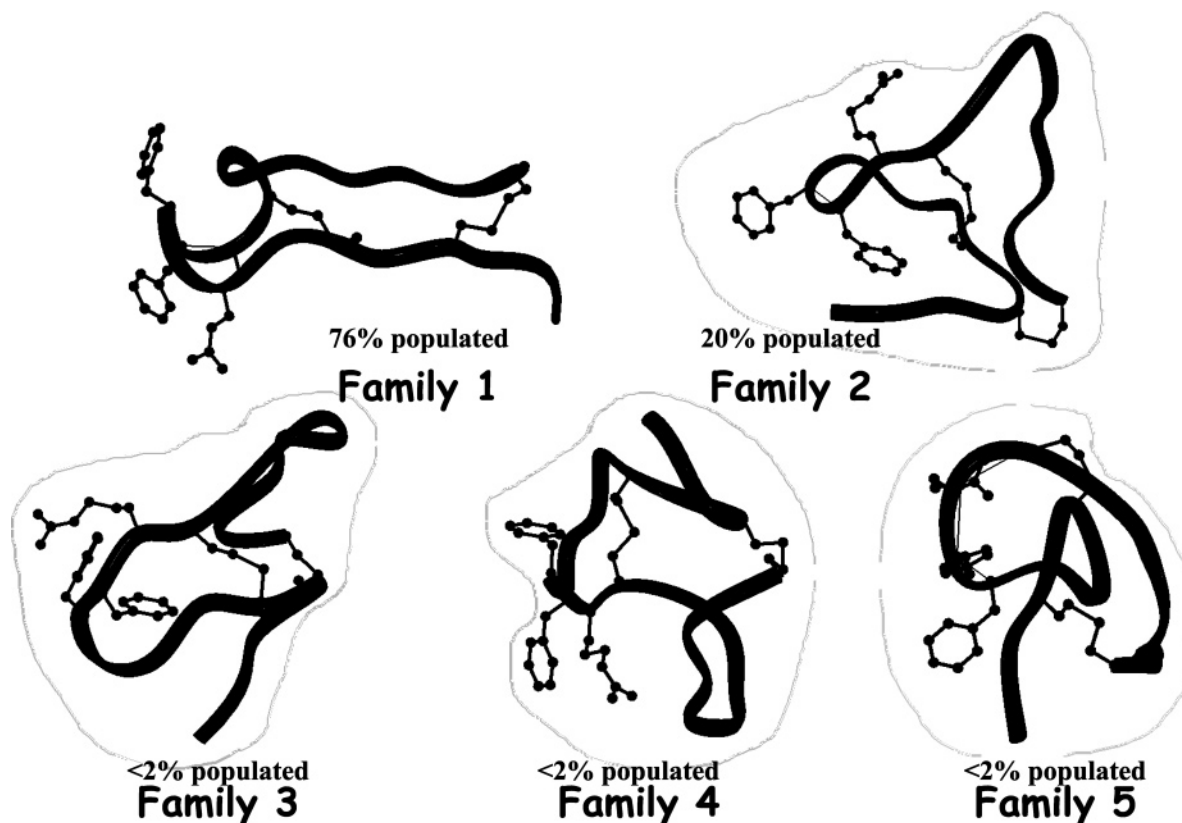
Figure 6. Illustration of the representative structure of five conformational families of peptide 1 after XCluster analysis. The percentage indicated represents the number of structures that are members of this conformational family. Energies derived after docking the conformational family into the mMC4R and performing ligand−receptor energy minimizations are as follows: family 1, −1730 kcal/mol; family 2, −1420 kcal/mol,; family 3, −1600 kcal/mol; family 4, −1640 kcal/mol; and family 5, −1380 kcal/mol. Family 1 possesses the most relative lowest energy conformations upon docking into the mMC4R. Upon docking of the peptide 1 conformational families into the 3D homology model of the mMC4R, it was identified that family 2 and family 5 (possessing the largest energy values) were sterically forbidden from docking into the mMC4R model (the ligand bisected the receptor transmembrane domain regions).

atoms (Figure 7A). Outside of the hAGRP(110−117) active site loop, the two structures diverge significantly, presumably because several disulfide bonds in this region are absent. The other four structural families of peptide 1 resulting from the cluster analysis had significantly larger (2.2−3.0 Å) RMSD values of the hAGRP(110−117) active site loop domain.

Docking of the Peptide 1 Representative Conformational Family Structures into a 3D Homology Molecular Model of the Mouse MC4R. We docked the representative structure from each of the five conformational family structures of peptide 1 (Figure 6) into a 3D homology molecular model of the mMC4R previously generated in our laboratory.[17] Since potentially all five of the NMR-derived structures of peptide 1 are theoretically biologically relevant solution conformations, we hypothesized that docking of these ligand structures into the mMC4 receptor homology model might provide a rationale for identifying the relevant "bioactive" conformational families that may be more pertinent than others. Of the five peptide 1 representative structures, families 1, 3, and 4 were docked into the mMC4R model and the intra- and intermolecular interactions of the ligand−MC4R complex are summarized in Table 4. The representative structures from families 2 and 5 (Figure 6) could not be docked into the receptor due to unfavorable steric interactions (the ligand bisected the mMC4R transmembrane domains).

The mMC4R-docked representative structure of family 1 has the lowest complex energy, and notably, family 1 also has the largest NMR-derived structural population (Figure 6). Figure 7B compares the peptide 1 conformational family 1 with the hAGRP(87−132) structure docked into the mouse MC4R, illustrating both the ligand structural similarities in the active loop cyclo-[Cys-Arg-Phe-Phe-Asn-Ala-Phe-Cys] and structural differences outside of this loop domain.

Discussion

Discovery and in vivo validation of the melanocortin pathway, specifically the MC3R, MC4R, POMC derived agonists, AGRP, and the agouti proteins (ASP and ASIP) as physiological regulators of weight and energy homeostasis, has resulted in targeting of this system for drug discovery efforts. In attempts to identify the molecular interactions between the endogenous AGRP antagonist and the MC4 receptor, several MC4 receptor mutagenesis studies have been performed.[19−25] Additionally, ligands have been designed, synthesized, and pharmacologically characterized, on the basis of the AGRP antagonist template, in attempts to identify hAGRP amino acids important for MC4R molecular recognition and antagonism.[12,13,15−18,26−31] The results of these previous studies have identified the following key information: (1) AGRP has both unique and identical putative MC4R binding and molecular recognition
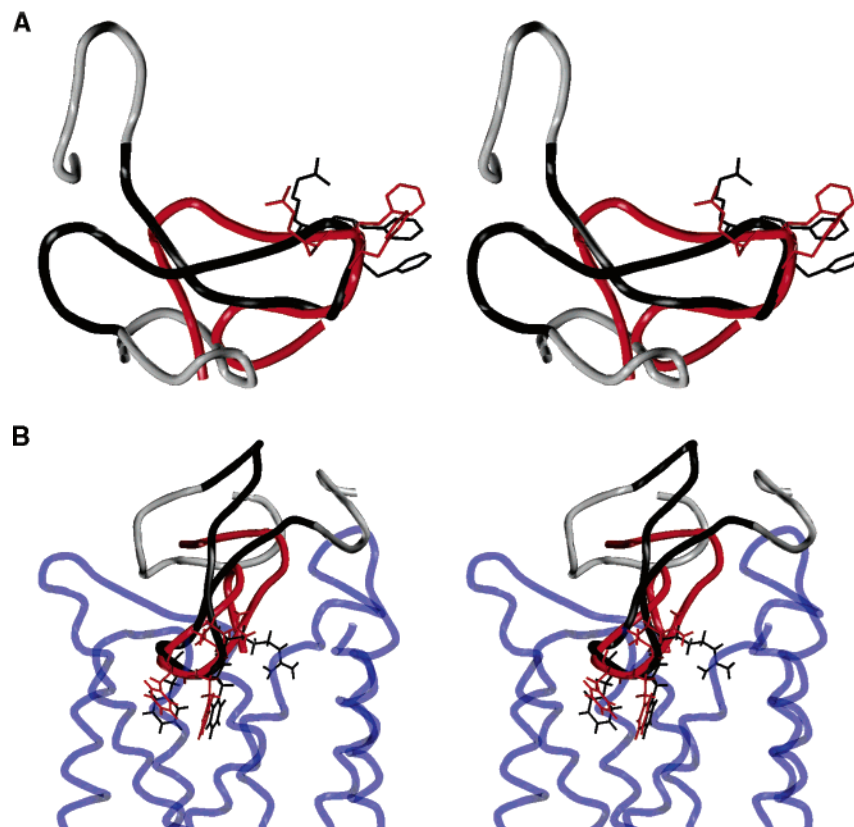
Figure 7. Stereoviews of the comparisons between the ligands and the ligands docked into the mouse MC4R. (A) The hAGRP(87−132) structure (shown in gray and black) as reported by Millhauser and colleagues is overlapped with peptide 1 (family 1, shown in red). The hAGRP(111−113) Arg-Phe-Phe amino acid side chains are illustrated. These structures represent the energy minimized ligand after they had been docked and minimized within the ligand−mMC4R complex. (B) The same hAGRP(87−132) and peptide 1 ligands as in panel A docked into the mMC4 receptor (blue). Only the mMC4R backbone atoms are presented (blue) for clarity.

interactions as the melanocortin agonists.[19,20,22] (2) Both radiolabeled antagonist I[125]-AGRP(87−132) and agonist I[125]-NDP-MSH can competitively displace AGRP(87−132), mini-AGRP, and truncated monocyclic analogues of hAGRP[10,12,15,17] with similar affinities. (3) AGRP is a competitive antagonist of melanocortin agonists (not an allosteric antagonist or modulator),[1,10,19,20] presenting strong experimental evidence that there are putative hAGRP residue interactions with the MC4R that are common with the melanocortin agonists. In attempts to identify a sequence of minimal length and minimal side chain cyclizations, yet still maintain nM mMC4R pharmacology, we synthesized and pharmacologically characterized two bicyclic peptides based upon the hAGRP template. Table 2 summarizes the ligand binding affinity (Figure 1) and functional activity at the melanocortin-1, -3, and -4 receptors (Figures 2 and 3). Figure 2 illustrates the MC3R and MC4R antagonist pharmacology of the bicyclic hAGRP peptide 1 at the melanocortin receptors. Figure 3 illustrates the MC1R agonist pharmacology of peptide 1, as compared to the endogenous agonist α-MSH.

Contrasts and Comparisons between AMW2−92 and hAGRP(87−132) Structures. Biophysical structural studies by Millhauser and colleagues have demonstrated that the AGRP(87−132) tertiary structure adopts an ICK fold.[11,12] Three hAGRP disulfide bridges (Cys87−Cys102, Cys94−Cys108, and Cys101−Cys119) and a three-stranded β-sheet (involving hAGRP residues 92−94, 106−110, and 117−121) are key structural motifs of this ICK type of fold. The β-sheet structure

contains a well-defined β-hairpin composed of the hAGRP 110−117 residues that also contains the functionally important hAGRP(111−113) Arg-Phe-Phe amino acids. This β-hairpin loop structure has been postulated to be essential for the antagonist activity of AGRP at the MC4 and MC3 receptors.[11,12,15] Moreover, this active loop is well-ordered in the AGRP(87−132) structure, with the hAGRP(111−113) Arg-Phe-Phe residues apparently well-poised to interact with the MC3 or MC4 receptor(s).

The central hAGRP(109−118) active loop (Tyr-cyclo-[Cys-Arg-Phe-Phe-Asn-Ala-Phe-Cys]-Tyr) is common to both peptide 1 and hAGRP(87−132), and is structurally similar (Figure 7A). However, the secondary structure outside of the core Tyr-cyclo[Cys-Arg-Phe-Phe-Asn-Ala-Phe-Cys]-Tyr hAGRP region possesses significant secondary structural differences between the peptide 1 and hAGRP(87−132) molecules (Figure 7A). The most obvious rationale for the differences between these structures can be attributed to changes in disulfide bonding and overall structure between the two molecules. Not surprisingly, there are chemical shift changes between the peptide 1 and hAGRP(87−132) analogues, primarily associated with differences in the number of disulfide bridges [peptide 1 has two disulfide bridges versus the five in hAGRP(87−132)], but also from significant changes in tertiary folding and substitution of the hAGRP Cys residues by α-aminobutyric acid (Abu) in peptide 1 (Table 2). [Abu was selected as a pseudo Cys isostere as it had been used successfully in studies presented by Amgen.[16]] The overall struc-

Table 4. Comparison of the Putative hAGRP(87−132) and Peptide 1 Conformational Families after Docking into the mMC4R and Energy Minimization of the Ligand−Receptor Complex

hAGRP(87−132) amino acid	mMC4R/hAGRP(87−132) putative interactions[a]	putative mMC4R/peptide 1 interactions		
		family 1	family 3	family 4
Arg89	hAGRPGlu92 backbone of Cys271 (EL3 adjacent to TM7 initiation)			
His91	Thr104 (EL1) backbone C=O of Asp103 (EL1) Tyr33 (N-termini adjacent to TM1 initiation)			
Glu92	hAGRPArg89			
Ser93	backbone of Cys271 (EL3 adjacent to TM7 initiation)			
Gln97	hAGRPAsn114 Asp181 (EL2 adjacent to TM5 initiation)			
Gln98	Asn266 (EL3)			
Asp103		bicyclic Arg120	bicyclic Arg120	bicyclic Tyr109 bicyclic Arg120
backbone of Ala106		Asp105 (EL1)		
backbone of Thr107		Asp105 (EL1)		Asp103 (EL1)
backbone of Cys108/Abu108		Asp105 (EL1)		
Tyr109	Asp114 (TM3)			bicyclic Asp103
backbone of Tyr109			Asp105 (EL1)	
Cys110		Gln107 (EL1)		
backbone of Cys110			Asp105 (EL1)	
Arg111	Glu92 (TM2) Asp114 (TM3) Asp118 (TM3)	Asp114 (TM3)[b] Asn115 (TM3) Asp118 (TM3)[b]	Asp114 (TM3)[b] Asn115 (TM3) Asp118 (TM3)[b]	Asp114 (TM3)[b] Asn115 (TM3)
Phe112	Phe176 (end of TM4 adjacent to EL2 initiation) Phe253 (TM6)	Phe176[b] (end of TM4 adjacent to EL2 initiation) Phe253 (TM6)[b]	Phe176[b] (end of TM4 adjacent to EL2 initiation)	Phe176[b] (end of TM4 adjacent to EL2 initiation) Phe253 (TM6)[b]
Phe113	Phe176 (end of TM4 adjacent to EL2 initiation) Phe193 (TM5) Phe253 (TM6) Phe254 (TM6)	Phe176[b] (end of TM4 adjacent to EL2 initiation) Phe193 (TM5)[b] Phe253 (TM6)[b]	Phe176[b] (end of TM4 adjacent to EL2 initiation)	Phe176[b] (end of TM4 adjacent to EL2 initiation) Phe193 (TM5)[b] Phe253 (TM6)[b]
Asn114	hAGRPGln97 Asp181 (EL2 adjacent to TM5 initiation)	backbone of Tyr260 (end of TM4 adjacent to EL2 initiation)	backbone of Leu257 (TM6)	bicyclic Arg120
Phe116	hAGRPTyr118			
backbone of Cys117			Asn277 (TM7)	
Tyr118	Asp105 (EL1) Gln107 (EL1) hAGRPPhe116	Thr104 (EL1)	backbone of Cys32 (TM1 initiation adjacent to N-termini)	Asp103 (EL1)
Arg120	Asp105 (EL1) Asp114 (TM3)	bicyclic Asp103	backbone of Phe272 (TM7 initiation adjacent to EL3 end) bicyclic Asp103	bicyclic Asp103 bicyclic Asn114
Lys121	hAGRPAsp103 Asp103 (EL1)	Asp103 (EL1)[b] Thr104 (EL1)		backbone of Cys269 (EL3) backbone of Cys271 (EL3)
backbone of Leu122		Gln35 (TM1 initiation adjacent to N-termini) Asn277 (TM7)		backbone of Cys269 (EL3)
Thr124	Thr110 (end of EL1 adjacent to TM3 initiation)			
Arg131	backbone of Ala106 (EL1)			
Thr132	Thr104 (EL1)			

[a] The putative hAGRP(87−132) interactions with the mMC4R have been previously reported (*17*). Blank spaces provided for putative ligand−MC4R interactions indicate that no interactions deemed significant were identified in the case of hAGRP(87−132), and/or that corresponding amino acids in the bicyclic ligands are absent. [b] Indicates an intermolecular interaction that is also observed in the putative hAGRP(87−132)−mMC4R interactions. Unless otherwise noted, the putative ligand−receptor side-chain to side-chain interactions are between the ligand and the mMC4R molecules.

tural similarity between AGRP(87−132) and peptide 1 is very low (Figure 7A), as might be expected by the inherent nature of these types of structure−function studies. However, superposition of the active loop containing hAGRP(111−116) Arg-Phe-Phe-Asn-Ala-Phe amino acids in the representative structure of the major conformational family of peptide 1, with the same region in AGRP(87−132), results in the relatively low RMSD of 1.4 Å for backbone atoms (Figure 7A). The nature of the turn in the hAGRP(111−116) Arg-Phe-Phe-Asn-Ala-Phe domain, however, is different between peptide 1 and the hAGRP(87−132) structures. In peptide 1 we find an inverse γ turn, defined by Rose et al. as the central residue of the turn with $\phi = -79°$ and $\psi = 69°$.[32] In peptide 1, the corresponding angles of Asn (of Phe-Asn-Ala) are $\phi = -82°$ and $\psi = 68°$. The same Asn (of Phe-Asn-Ala) residues in AGRP(87−132) have peptide backbone torsion angles of $\phi = -155°$ and $\psi = 76°$. We attribute these secondary structural changes between peptide 1 and hAGRP(87−132) to differences in disulfide bonds and conformational flexibility in the two molecules.

Putative hAGRP and Peptide 1 Ligand−Melanocortin-4 Receptor Interactions. Homology molecular modeling of GPCRs using the structural information provided by the GPCR rhodopsin[33] is a common approach in attempts to identify putative ligand−receptor interactions using a variety of computational techniques. While it is desirable to utilize an X-ray crystal structure or NMR based structural data for rational based drug design, for GPCRs this is an extremely daunting task as it is a membrane spanning protein and the lipid bilayer of the cell is required for receptor function. Thus, homology molecular modeling of GPCRs is the only currently accessible technique for a "pseudo" GPCR structure based design strategy.[34] While this GPCR homology molecular modeling approach is thwarted by many poor assumptions and low resolution starting structures, nonetheless, it provides a theoretical strategy to develop specific putative ligand−receptor interaction hypotheses that could be developed and experimentally tested that might otherwise not be available.

On the basis of differences in antagonist ligand melanocortin receptor pharmacology and the NMR derived structures, we compared the mMC4R docked ligand interactions of peptide 1 and hAGRP(87−132) in attempts to identify any putative ligand−receptor interaction differences that could be identified to potentially account for the 80-fold difference in antagonist potency and be tested in future experiments (Figure 7B). Table 4 summarizes the putative ligand−receptor interactions for hAGRP(87−132) identified from our previous study,[17] and conformational families 1, 3, and 4 of the bicyclic hAGRP analogue **1**. Although these comparisons are based upon relatively low resolution experimental structures, and possess many inherent experimental assumptions associated with 3D GPCR homology molecular modeling, we nevertheless propose that this approach may lead to new experimental design strategies to elucidate putative AGRP−MC4 receptor interactions. With these caveats in mind, comparisons of the putative ligand−MC4R interaction differences between the hAGRP(87−132) and peptide 1 molecules

were undertaken and two main postulated differences between the hAGRP(87−132) and peptide 1 ligand−mMC4R were identified and are discussed below.

The monocyclic hAGRP(110−117) central domain has been identified in hAGRP to possess the minimal structural information to bind and competitively antagonize the mouse and human MC4 receptors[13,14] and contains the key Arg-Phe-Phe amino acids important for antagonism of the melanocortin receptors.[13] Focusing on these key Arg-Phe-Phe hAGRP(111−113) amino acids, as summarized in Table 4, the docked structures of peptide 1 all maintain similar putative ligand−receptor interactions. Additionally, after ligand−receptor energy minimization of the peptide 1−mMC4R complex, peptide 1 Arg111 residue putatively interacts with an additional mMC4R Asn115 amino acid whose interaction was not observed for hAGRP(87−132).[17] It appears that this mMC4R Asn115 interaction with peptide 1 may be an alternative putative contact compared with the hAGRP(87−132)−mMC4RGlu92 interaction, perhaps accounting for the decrease in peptide 1 ligand antagonist potency.

The importance of the hAGRP(87−132) Arg120 amino acid for putative ligand−receptor interactions has been postulated in elongation studies of the hAGRP(109−118) monocyclic peptide.[15] On the basis of the MC4R homology molecular modeling and hAGRP(87−132) ligand docking studies,[17] it was identified that this hAGRP Arg(120) amino acid putatively interacts with the highly conserved melanocortin Asp114 residue in TM3. Previous receptor mutagenesis studies of both the MC1R and MC4R (various species) have resulted in the identification that this TM3 Asp114 receptor residue is important for melanocortin ligand−receptor interactions.[19,20,35,36] Comparison of the docked hAGRP(87−132) and the bicyclic peptide 1 structural families (Table 4) resulted in the absence of this putative hAGRP Arg120−mMC4R Asp113 interaction for peptide 1 ligands. Additionally, differences between the putative hAGRPArg111 and peptide 1 Arg111 interactions with the mMC4R were observed. The differences between these AGRP ligands may account for the decreased antagonist potency of peptide 1, although this speculation remains to be verified experimentally. Other putative ligand−mMC4R interaction differences outside the Arg-Phe-Phe(111−113) motif are observed for hAGRP(87−132) and peptide 1, as summarized in Table 4, that may also attribute to the decreased potency of peptide 1. Given the sequence similarity of mouse and human MC4 receptors, it is likely that these observations will also by applicable to the design of novel antagonists for the human receptor isoform.

Summary

In the studies reported herein, we have synthesized and pharmacologically characterized two bicyclic peptides that result in antagonism of the MC3 and MC4 receptors. The most potent 22 amino acid bicyclic peptide 1 possessed equipotent mMC4R binding (within experimental error), as compared with the hAGRP(87−132) ligand that possesses five disulfide bridges and 46 amino acids. Albeit peptide 1 is an 80-fold less potent antagonist than hAGRP(87−132) at the mMC4R. NMR structural studies were initiated to identify the solu-

tion structure(s) of peptide 1 and determine the extent of conformational homogeneity as compared to the hAGRP(87−132) NMR structure presented by Millhauser et al. The conclusion from these structural analyses is that hAGRP(87−132) and the bicyclic peptide 1 structures differ significantly outside the core hAGRP(109−118) decapeptide region that is minimally required for MC4R antagonism (μM), but overlap considerably in this core hAGRP decapeptide domain. To take this study an additional step, we docked the five possible conformational families of peptide 1 into a homology molecular model of the mouse MC4R, and discovered that two of the five families were sterically forbidden from "docking" into the receptor (the ligand bisected the receptor TM domains). Furthermore, we attempted to use this latter experiment as a tool to identify putative ligand−receptor interactions that might explain differences in decreased antagonist potency of peptide 1 (80-fold) as compared with hAGRP(87−132), as it is well recognized that specific receptor residues are different for ligand binding and receptor functional activity. Thus, these combinations of experimental and theoretical approaches have resulted in the generation of specific hypotheses related to hAGRP−mMC4R putative ligand−receptor interactions that can be experimentally tested in future studies.

Experimental Section

Peptides Synthesis. hAGRP(87−132) was purchased from Peptides International (Louisville, KY), and mini-hAGRP was synthesized in our laboratory[17] as previously reported by Jackson et al.[12] The bicyclic peptides were synthesized using standard Fmoc methodology.[37,38] All amino acids and reagents were purchased from commercial sources. The Nα 9-fluorenylmethoxycarbonyl (Fmoc) protected amino acids Cys(Acm), Cys(Trt), α-aminobutyric acid (Abu), Asp(tBu), Glu(tBu) Thr(tBu), Ser(tBu), Tyr(tBu), Arg(Pbf), Lys(tBu), His(Trt), Phe, Asn(Trt), Gln(Trt), Val, Gly, Pro, Ala, and Leu were utilized. Benzotriazol-1-yl-oxy-tris(dimethylamino) phosphonium hexafluorophosphate (BOP) and 1-hydroxybenzotriazole (HOBt) were used as coupling reagents. Dichloromethane (DCM), glacial acetic acid, methanol, acetonitrile, anhydrous ethyl ether, *N,N*-dimethylformamide (DMF), trifluoroacetic acid (TFA), dimethyl sulfoxide (DMSO), piperidine, phenol, *N,N*-diisopropylethylamine (DIEA), triisopropylsilane (TIS), and 1,2-ethanedithiol (EDT) were used as reagents or solvents in the syntheses. All reagents and chemicals were ACS grade or better and were used without further purification.

The peptides were assembled on 9-fluorenylmethoxycarbonyl-leucine-*p*-alkoxybenzyl alcohol resin (Fmoc-Leu-Wang resin) (0.73 mequiv/g substitution) purchased from Peptides International (Louisville, KY). The synthesis (0.26 mmol scale) was performed using a manual synthesis reaction vessel. Each synthetic cycle consisted of the following steps: (i) removal of the Nα Fmoc group by 20% piperidine in DMF (1 × 2 min, 1 × 20 min) (ii) single 2 h coupling of Fmoc-amino acid (3 equiv) using BOP (3 equiv), HOBt (3 equiv), and DIEA (6 equiv) in DMF and repeated until the peptide synthesis was complete. The presence or absence of the Nα free amino group was monitored using the Kaiser test.[39] After the completed synthesis, the peptides were cleaved from the resin and deprotected using a cleavage cocktail consisting of 82.5% TFA, 5% H$_2$O, 5% EDT, 5% phenol, and 2.5% TIS for 3 h at room temperature. After cleavage and side chain deprotection, the solution was concentrated and the peptide was precipitated and washed using cold (4 °C), anhydrous diethyl ether. The crude, linear peptides were purified by reversed-phase HPLC using a Shimadzu chromatography system with a photodiode array detector and a semipreparative RP-HPLC C18 bonded silica column (Vydac 218TP1010, 1.0 × 25 cm). Peptide 1 was

purified using a gradient of 33% to 43% acetonitrile/water 0.1% TFA over 10 min at a flow rate of 5.0 mL/min. Peptide 2 was purified using a gradient to 30% to 36% acetonitrile/water 0.1% TFA over 10 min at a flow rate of 5.0 mL/min.

To ensure the correct disulfide pairing, the thiol groups were protected with trityl groups (which are removed by the cleavage cocktail) and Acm groups, which are stable for both acidic and basic conditions.[40] The purified Acm-protected linear peptides were oxidized to the disulfide form by reaction with 5% DMSO in H$_2$O. The peptides were dissolved at a concentration of 0.37 mg/mL, and the solution was allowed to react at 20 °C. The oxidation process was monitored using analytical RP-HPLC for the disappearance of the linear peptide [k'(peptide 1) = 7.8, k'(peptide 2) = 7.2] and formation of the cyclized product [k'(peptide 1) = 7.1, k'(peptide 2) = 6.1] in 10% to 90% acetonitrile/water 0.1% TFA in 35 min at a flow rate of 1.5 mL/min. After the oxidation reaction was complete, the solution was lyophilized and the peptide was used for the next step without purification. The second disulfide bridge was formed by oxidation with iodine (I$_2$).[41] The peptide was dissolved in AcOH−H$_2$O (4:1) to a final concentration of 2 mg/mL, and the I$_2$ in MeOH (10 equiv) solution was added in one portion to the dissolved peptide. The reaction mixture was mixed in the dark at 20 °C. After 2 h, the mixture was diluted to twice the volume with water and excess iodine was removed by extraction with carbon tetrachloride. The aqueous phase was lyophilized, and the peptide was purified by RP-HPLC. The purified peptides were at least >98% pure as determined by RP-HPLC in two diverse solvent systems and had the correct molecular mass (University of Florida Protein Core Facility), Table 1. The overall yields for peptide 1 and peptide 2 are 2.7% and 2.9%, respectively, based upon the original resin loading capacity.

NMR Spectroscopy. Peptide NMR samples were prepared by dissolving 3 mg of peptide 1 in 600 μL 95% H$_2$O/5% D$_2$O, adjusting the pH to 5.5, and adding DSS as an internal standard (0.0 ppm). NMR data were collected at 30 °C with 600 and 750 MHz Bruker Avance spectrometers in the Advanced Magnetic Resonance Imaging and Spectroscopy (AMRIS) facility at the University of Florida. Standard proton-based 2D NMR data were collected, processed, and analyzed as described previously.[18] NOESY data were collected at both 100 and 400 ms mixing times, and proton−proton distances were obtained from the 400 ms dataset.

Computer-Assisted Molecular Modeling (CAMM). Experimental NMR restraints from NOEs were classified as strong, medium, or weak with upper limits 3.5 Å, 4.5 Å, and 5.0 Å, respectively. Sequential and medium-range (up to $i \rightarrow i + 4$) NOE cross-peaks were used in the modeling, which was performed using Insight II and Discover software (Accerlys, San Diego, CA). The peptide model was built in a fully extended conformation, and a brief dynamics simulation was used to relax the coordinates. All restrained molecular dynamics (RMD) simulations were run in a vacuum with a dielectric constant of 4.0 and at 500 K and used the cvff force field with no cross terms. In order to prevent the ring structures from getting trapped in local minima, five unambiguous medium-range NMR restraints were added as pseudopotentials for 5 ns of RMDs before forming disulfide bonds. Following the initial 5 ns RMD trajectory, the correct cysteine residues were oriented next to each other, and disulfide bonds were manually formed. The peptide 1 hAGRP bicyclic structure was then energy minimized with no restraints. All unambiguous NOE restraints (16 sequential and 5 medium-range) were then applied to the energy minimized bicyclic structure, and a RMD simulation was run for 20 ns. At the end of this simulation, one additional ambiguous NOE was resolved by looking at the structures, and it was added to the unambiguous NOEs, and another RMD simulation was run for 17 ns. Next, structures from 167 equally spaced points along the dynamics trajectory were energy minimized with the complete set of NMR restraints and analyzed.

The energy minimized structures were grouped into families using the XCluster program[42] by comparison of backbone

dihedral angles (ϕ and ψ) in the ring containing the active hAGRP(111−116) Arg-Phe-Phe-Asn-Ala-Phe sequence. Cluster analysis yielded five families (Figure 6), and representative structures from each family, selected by XCluster, were used for further analysis. Each representative structure was superimposed using InsightII with coordinates from the NMR structure (PDB file 1HYK) from the Millhauser's laboratory.[11,29] Each conformational family representative structure was additionally docked into the putative active site model of MC4R.[17]

Homology Molecular Modeling of the Melanocortin-4 Receptor−Ligand Complex. The homology model of the hAGRP(87−132)−melanocortin-4 receptor complex, as previously described,[17] was used as a starting point to dock the five representative structures of peptide 1 bicyclic peptide (Figure 6). For experimental details on the development of the mMC4R homology model, see Wilczynski et al.[17] Granted this is only a theoretical model based upon a large number of assumptions and low resolution biophysical data (rhodopsin starting structure), and must be evaluated in the context of these caveats, nonetheless it can be a valuable tool to generate specific ligand−receptor hypotheses that can then be tested experimentally in the future, in the absence of X-ray crystal structures of peptide hormone GPCRs.

Docking of Peptide 1 Representative Conformational Family Structures into a 3D Homology Molecular Model of the mouse MC4R. The NMR and CAMM generated bicyclic peptide 1 structures representing the different conformational families illustrated in Figure 6 were "docked" into a mMC4 receptor homology molecular model derived from previous studies in our laboratory.[17] On the basis of the knowledge that the hAGRP(111−113) Arg-Phe-Phe residues are crucial for the physiological function of hAGRP as a melanocortin receptor antagonist,[11−13] the hAGRP(111−113) Arg-Phe-Phe amino acid α carbons of peptide 1 were superposed onto the identical Arg-Phe-Phe α carbons of the docked structure of the hAGRP(87−132) ligand.[17] The torsion angles of hAGRP(111−113) Arg-Phe-Phe amino acid side chains were identified as predominantly in trans and gauche (+,−) conformations, as theoretically predicted. All five peptide 1-MC4R complex structures were checked carefully before an energy minimized conformational search was performed. Interestingly the approach of docking theoretically possible ligand structures, based upon NMR and CAMM, into the 3D homology model of the receptor resulted in the identification of two sterically forbidden ligand structures, conformational families 2 and 5 (Figure 6), that were excluded from further ligand-docking studies. The disulfide loop connecting the hAGRP Cys102 to Cys119 residues of the bicyclic peptide 1 ligand representative structure from family 2 passed through the extracellular loop 2 (EL2) backbone of the melanocortin-4 receptor, which is a sterically forbidden interaction. Similarly, the disulfide loop connecting the hAGRP Cys102 to Cys119 residues of the bicyclic peptide 1 ligand representative structure from family 5 passed through the upper transmembrane-7 (TM7) backbone of the melanocortin-4 receptor, also a sterically forbidden interaction.

Cell Culture and Transfection. HEK-293 cells were maintained in Dulbecco's modified Eagle's medium (DMEM) with 10% fetal calf serum and seeded 1 day prior to transfection at 1 to 2×10^6 cell/100 mm dish. Melanocortin receptor DNA in the pCDNA$_3$ expression vector (20 μg) was transfected using the calcium phosphate method. Stable receptor populations were generated using G418 selection (1 mg/mL) for subsequent bioassay analysis.

cAMP Based Functional Bioassay. HEK-293 cells stably expressing the melanocortin receptors were transfected with 4 μg CRE/β-galactosidase reporter gene as previously described.[19,43,44] Briefly, 5000 to 15000 post-transfection cells were plated into 96 well Primera plates (Falcon) and incubated overnight. Forty-eight hours post-transfection the cells were stimulated with 100 μL peptide (10^{-4}−10^{-12} M) or forskolin (10^{-4} M) control in assay medium (DMEM containing 0.1 mg/mL BSA and 0.1 mM isobutylmethylxanthine) for 6 h. The

assay medium was aspirated, and 50 μL of lysis buffer (250 mM Tris-HCl pH = 8.0 and 0.1% Triton X-100) was added. The plates were stored at −80 °C overnight. The plates containing the cell lysates were thawed the following day. Aliquots of 10 μL were taken from each well and transferred to another 96 well plate for relative protein determination. To the cell lysate plates, 40 μL phosphate-buffered saline with 0.5% BSA was added to each well. Subsequently, 150 μL of substrate buffer (60 mM sodium phosphate, 1 mM MgCl$_2$, 10 mM KCl, 5 mM β-mercaptoethanol, 2 mg/mL ONPG) was added to each well and the plates were incubated at 37 °C. The sample absorbance, OD$_{405}$, was measured using a 96 well plate reader (Molecular Devices). The relative protein was determined by adding 200 μL of 1:5 dilution Bio Rad G250 protein dye:water to the 10 μL cell lysate sample taken previously, and the OD$_{595}$ was measured on a 96 well plate reader (Molecular Devices). Data points were normalized to both the relative protein content and nonreceptor dependent forskolin stimulation. The antagonistic properties of these compounds were evaluated by the ability of these ligands to competitively displace the MTII agonist (Bachem) in a dose-dependent manner, at up to 10 μM concentrations.[19] The pA_2 values were generated using the Schild analysis method.[45]

Data Analysis. EC$_{50}$ and pA_2 values represent the mean of duplicate experiments performed in triplet, quadruplet, or more independent experiments. EC$_{50}$ and pA_2 estimates, and their associated standard errors, were determined by fitting the data to a nonlinear least-squares analysis using the PRISM program (v3.0, GraphPad Inc.). The ligands were assayed as TFA salts.

Competitive Displacement Binding Assays. hAGRP-(87−132) Iodination. [^{125}I]hAGRP(87−132) was prepared using a modified chloramine-T method as previously described by Yang et al.[10] Using 50 mM sodium phosphate buffer pH 7.4 as the reaction buffer, ^{125}I-Na (0.5 mCi, Amersham Life Sciences, Inc., Arlington Heights, IL) was added to 20 μg of hAGRP(87−132) (Peptides International, Louisville, KY) in 5 μL of buffer. To initiate the reaction, 10 μL of a 2.4 mg/mL solution of chloramine-T (Sigma Chemical Co., St. Louis, MO) was added for 15 s with gentle agitation. This reaction was terminated by the addition of 50 μL of a 4.8 mg/mL solution of sodium metabisulfite (Sigma Chemical Co.) for 20 s with gentle agitation. The reaction mixture was then diluted with 200 μL of 10% bovine serum albumin and the resultant mixture layered on a Bio-Gel P6 (Bio-Rad labs, Hercules, CA) column (1.0 × 50 cm Econocolumn, Bio-Rad Labs) for separation by size exclusion chromatography using 50 mM sodium phosphate buffer, pH 7.4 as column eluant. Fifteen drop fractions (ca. 500 μL) were collected into glass tubes containing 500 μL of 1% BSA. Each fraction was then counted on the Apex Automatic Gamma Counter (ICN Micromedic Systems Model 28023, Huntsville, AL with RIA AID software, Robert Maciel Associates, Inc., Arlington, MA) to determine peak ^{125}I incorporation fractions.

Receptor Competitive Displacement Binding Studies. HEK-293 cells stably expressing the mouse MC3 and MC4 receptors were maintained as described above. One day preceding the experiment, $0.1−0.3 \times 10^6$ cells/well were plated into Primera 24 well plates (Falcon). The peptides were used to competitively displace the I^{125}-radiolabeled hAGRP(87−132) (100000 cpm/well). The ligands were assayed as TFA salts. Dose−response curves (10^{-6} to 10^{-12} M) of hAGRP(87−132) and IC$_{50}$ values were generated and analyzed by nonlinear least-squares analysis[46] and the PRISM program (v3.0, Graph-Pad Inc.). The percent total specific binding was determined based upon the nonspecific values obtained using 10^{-6} M hAGRP(87−132) and the hAGRP(87−132) dose−response curves as controls. Each experiment was performed using duplicate data points and repeated in at least two independent experiments. The standard deviation errors of the mean were derived from the average percent specific binding values from at least two independent experiments and using the PRISM program (v3.0, GraphPad Inc.).

Acknowledgment. This work has been supported by NIH Grants R01DK57080 (C.H.-L.), R01DK64250 (C.H.-L.), 5P41RR016105 (A.S.E.), and an NSF CAREER award (A.S.E.). C.H.-L. is a recipient of an American Diabetes Association Research Award. A.W. is a recipient of an American Heart Association Postdoctoral Fellowship.

Appendix

Abbreviations. mMC1R, mouse melanocortin-1 receptor; mMC3R, mouse melanocortin-3 receptor; mMC4R, mouse melanocortin-4 receptor; mMC5R, mouse melanocortin-5 receptor; Abu and U, α-aminobutyric acid; AGRP, agouti-related protein; GPCR, G-protein coupled receptor; ASP, mouse form of the agouti protein; α-MSH, α-melanocyte stimulating hormone; POMC, proopiomelanocortin; cAMP, cyclic 3′,5′-adenosine monophosphate; HEK-293 cells, human embryonic kidney cells; NMR, nuclear magnetic resonance; NOESY, nuclear Overhauser effect spectroscopy; TOCSY, total correlation spectroscopy; CAMM, computer assisted molecular modeling; RMSD, root-mean-square deviation; RMD, restrained molecular dynamics; TM, transmembrane.

References

 (1) Ollmann, M. M.; Wilson, B. D.; Yang, Y.-K.; Kerns, J. A.; Chen, Y.; et al. Antagonism of Central Melanocortin Receptors in Vitro and in Vivo by Agouti-Related Protein. *Science* **1997**, *278*, 135–138.
 (2) Huszar, D.; Lynch, C. A.; Fairchild-Huntress, V.; Dunmore, J. H.; Smith, F. J.; et al. Targeted Disruption of the Melanocortin-4 Receptor Results in Obesity in Mice. *Cell* **1997**, *88*, 131–141.
 (3) Nijenhuis, W. A.; Oosterom, J.; Adan, R. A. AGRP(83–132) Acts as an Inverse Agonist on the Human-Melanocortin-4 Receptor. *Mol. Endocrinol.* **2001**, *15*, 164–171.
 (4) Haskell-Luevano, C.; Monck, E. K. Agouti-related Protein (AGRP) Functions as an Inverse Agonist at a Constitutively Active Brain Melanocortin-4 Receptor. *Regul. Pept.* **2001**, *99*, 1–7.
 (5) Chai, B. X.; Neubig, R. R.; Millhauser, G. L.; Thompson, D. A.; Jackson, P. J.; et al. Inverse Agonist Activity of Agouti and Agouti-Related Protein. *Peptides* **2003**, *24*, 603–609.
 (6) Gunn, T. M.; Miller, K. A.; He, L.; Hyman, R. W.; Davis, R. W.; et al. The Mouse Mahogany Locus Encodes a Transmembrane Form of Human Attractin. *Nature* **1999**, *398*, 152–156.
 (7) Nagle, D. L.; McGrail, S. H.; Vitale, J.; Woolf, E. A.; Dussault, B. J., Jr.; et al. The Mahogany Protein is a Receptor Involved in Suppression of Obesity. *Nature* **1999**, *398*, 148–152.
 (8) He, L.; Gunn, T. M.; Bouley, D. M.; Lu, X. Y.; Watson, S. J.; et al. A Biochemical Function for Attractin in Agouti-induced Pigmentation and Obesity. *Nat. Genet.* **2001**, *27*, 40–47.
 (9) Reizes, O.; Lincecum, J.; Wang, Z.; Goldberger, O.; Huang, L.; et al. Transgenic Expression of Syndecan-1 Uncovers a Physiological Control of Feeding Behavior by Syndecan-3. *Cell* **2001**, *106*, 105–116.
(10) Yang, Y.-K.; Thompson, D. A.; Dickinson, C. J.; Wilken, J.; Barsh, G. S.; et al. Characterization of Agouti-Related Protein Binding to Melanocortin Receptors. *Mol. Endocrinol.* **1999**, *13*, 148–155.
(11) McNulty, J. C.; Thompson, D. A.; Bolin, K. A.; Wilken, J.; Barsh, G. S.; et al. High-Resolution NMR Structure of the Chemically-Synthesized Melanocortin Receptor Binding Domain AGRP(87–132) of the Agouti-Related Protein. *Biochemistry* **2001**, *40*, 15520–15527.
(12) Jackson, P. J.; McNulty, J. C.; Yang, Y. K.; Thompson, D. A.; Chai, B.; et al. Design, Pharmacology, and NMR Structure of a Minimized Cystine Knot with Agouti-Related Protein Activity. *Biochemistry* **2002**, *41*, 7565–7572.
(13) Tota, M. R.; Smith, T. S.; Mao, C.; MacNeil, T.; Mosley, R. T.; et al. Molecular Interaction of Agouti Protein and Agouti-Related Protein with Human Melanocortin Receptors. *Biochemistry* **1999**, *38*, 897–904.
(14) Haskell-Luevano, C.; Monck, E. K.; Wan, Y. P.; Schentrup, A. M. The Agouti-related Protein Decapeptide (Yc[CRFFNAFC]Y) Possesses Agonist Activity at the Murine Melanocortin-1 Receptor. *Peptides* **2000**, *21*, 683–689.
(15) Joseph, C. G.; Bauzo, R. M.; Xiang, Z.; Shaw, A. M.; Millard, W. J.; et al. Elongation Studies of the Human Agouti-Related Protein (AGRP) Core Decapeptide (Yc[CRFFNAFC]Y) Results in Antagonism at the Mouse Melanocortin-3 Receptor. *Peptides* **2003**, *27*, 263–270.
(16) Jarosinski, M. A.; Dodson, S. W.; Harding, B. J.; Hale, C.; McElvain, M.; et al. Design and Synthesis of Simplified AGRP(65-112) Analogues: Protein-Mimetics with Affinity at the Melanocortin Receptors. Presented at the 2nd International and 17th American Peptide Symposium, San Diego, CA, 2001; Poster 322.
(17) Wilczynski, A.; Wang, X. S.; Joseph, C. G.; Xiang, Z.; Bauzo, R. M.; et al. Identification of Putative Agouti-Related Protein(87–132)-Melanocortin-4 Receptor Interactions by Homology Molecular Modeling and Validation Using Chimeric Peptide Ligands. *J. Med. Chem.* **2004**, *47*, 2194–2207.
(18) Thirumoorthy, R.; Holder, J. R.; Bauzo, R. M.; Richards, N. G. J.; Edison, A. S.; et al. Novel Agouti-related Protein (AGRP) Based Melanocortin-1 Receptor Antagonist. *J. Med. Chem.* **2001**, *44*, 4114–4124.
(19) Haskell-Luevano, C.; Cone, R. D.; Monck, E. K.; Wan, Y.-P. Structure Activity Studies of the Melanocortin-4 Receptor by In Vitro Mutagenesis: Identification of Agouti-Related Protein (AGRP), Melanocortin Agonist and Synthetic Peptide Antagonist Interaction Determinants. *Biochemistry* **2001**, *40*, 6164–6179.
(20) Yang, Y.; Fong, T. M.; Dickinson, C. J.; Mao, C.; Li, J. Y.; et al. Molecular Determinants of Ligand Binding to the Human Melanocortin-4 Receptor. *Biochemistry* **2000**, *39*, 14900–14911.
(21) Yang, Y.; Dickinson, C. J.; Zeng, Q.; Li, J. Y.; Thompson, D. A.; et al. Contribution of Melanocortin Receptor Exoloops to Agouti-related Protein Binding. *J. Biol. Chem.* **1999**, *274*, 14100–14106.
(22) Yang, Y.; Chen, M.; Lai, Y.; Gantz, I.; Yagmurlu, A.; et al. Molecular Determination of Agouti-Related Protein Binding to Human Melanocortin-4 Receptor. *Mol. Pharmacol.* **2003**, *64*, 94–103.
(23) Tao, Y. X.; Segaloff, D. L. Functional Characterization of Melanocortin-4 Receptor Mutations Associated with Childhood Obesity. *Endocrinology* **2003**, *144*, 4544–4551.
(24) Nickolls, S. A.; Cismowski, M. I.; Wang, X.; Wolff, M.; Conlon, P. J.; et al. Molecular Determinants of Melanocortin 4 Receptor Ligand Binding and MC4/MC3 Receptor Selectivity. *J. Pharmacol. Exp. Ther.* **2003**, *304*, 1217–1227.
(25) VanLeeuwen, D.; Steffey, M. E.; Donahue, C.; Ho, G.; MacKenzie, R. G. Cell Surface Expression of the Melanocortin-4 Receptor is Dependent on a C-Terminal Di-Isoleucine Sequence at Codons 316/317. *J. Biol. Chem.* **2003**, *278*, 15935–15940.
(26) Joseph, C. G.; Wilczynski, A. M.; Holder, J. R.; Bauzo, R. M.; Scott, J. W.; et al. Chimeric NDP-MSH and MTII Melanocortin Peptides with Agouti-Related Protein (AGRP) Arg-Phe-Phe Amino Acids Possess Agonist Melanocortin Receptor Activity. *Peptides* **2003**, *24*, 1899–1908.
(27) Joseph, C. G.; Bauzo, R. M.; Scott, J. W.; Haskell-Luevano, C. Stereochemical Inversion Studies of a Monocyclic hAGRP(103-122) Peptide. In *Peptide Revolution: Genomics, Proteomics & Therapeutics, Proceedings of the 18th American Peptide Symposium*; Chorev, M., Sawyer, T. K., Eds.; Kluwer Academic Publishers: The Netherlands, in press.
(28) Arasasingham, P. N.; Fotsch, C.; Ouyang, X.; Norman, M. H.; Kelly, M. G.; et al. Structure–Activity Relationship of (1-Aryl-2-Piperazinylethyl)Piperazines: Antagonists for the AGRP/Melanocortin Receptor Binding. *J. Med. Chem.* **2003**, *46*, 9–11.
(29) Bolin, K. A.; Anderson, D. J.; Trulson, J. A.; Thompson, D. A.; Wilken, J.; et al. NMR Structure of a Minimized Human Agouti Related Protein Prepared by Total Chemical Synthesis. *FEBS Lett.* **1999**, *451*, 125–131.
(30) Thompson, D. A.; Chai, B. X.; Rood, H. L.; Siani, M. A.; Douglas, N. R.; et al. Peptoid Mimics of Agouti Related Protein. *Bioorg. Med. Chem. Lett.* **2003**, *13*, 1409–1413.
(31) Wilson, K. R.; Wilczynski, A. M.; Scott, J. W.; Bauzo, R. M.; Haskell-Luevano, C. A Novel AGRP-Melanocortin Peptide Chimeric Library. In *Peptide Revolution: Genomics, Proteomics & Therapeutics, Proceedings of the 18th American Peptide Symposium*; Chorev, M., Sawyer, T. K., Eds.; Kluwer Academic Publishers: The Netherlands, in press.
(32) Rose, G. D.; Gierasch, L. M.; Smith, J. A. Turns in Peptides and Proteins. *Adv. Protein Chem.* **1985**, *37*, 1–109.
(33) Palczewski, K.; Kumasaka, T.; Hori, T.; Behnke, C. A.; Motoshima, H.; et al. Crystal Structure of Rhodopsin: A G protein-coupled Receptor. *Science* **2000**, *289*, 739–745.
(34) Bondensgaard, K.; Ankersen, M.; Thogersen, H.; Hansen, B. S.; Wulff, B. S.; et al. Recognition of Privileged Structures by G-Protein Coupled Receptors. *J. Med. Chem.* **2004**, *47*, 888–899.
(35) Lu, D.; Väge, D. I.; Cone, R. D. A Ligand-Mimetic Model for Constitutive Activation of the Melanocortin-1 Receptor. *Mol. Endocrinol.* **1998**, *12*, 592–604.
(36) Yang, Y.-K.; Dickinson, C.; Haskell-Luevano, C.; Gantz, I. Molecular Basis for the Interaction of [Nle4, DPhe7] Melanocyte Stimulating Hormone with the Human Melanocortin-1 Receptor (Melanocyte α-MSH Receptor). *J. Biol. Chem.* **1997**, *272*, 23000–23010.

(37) Carpino, L. A.; Han, G. Y. The 9-Fluorenylmethyloxycarbonyl Amino-Protecting Group. *J. Org. Chem.* **1972**, *37*, 3404−3409.

(38) Chang, C.; Meienhofer, J. Solid-Phase Peptide Synthesis Using Mild Base Cleavage of Nα-Fluorenylmethyloxycarbonyl Amino Acids, Exemplified by a Synthesis of Dihydrosomatostatin. *Int. J. Pept. Protein Res.* **1978**, *11*, 246−249.

(39) Kaiser, E.; Colescott, R. L.; Bossinger, C. D.; Cook, P. I. Color Test for Detection of Free Terminal Amino Groups in the Solid-Phase Synthesis of Peptides. *Anal. Biochem.* **1970**, *34*, 595−598.

(40) Veber, D.; Milkowski, J. D.; Varga, S. L.; Denkewalter, R. G.; Hirshmann, R. A Novel Thiol Protecting Group for Cysteine. *J. Am. Chem. Soc.* **1972**, *94*, 5456−5461.

(41) Zamborelli, T. J.; Dodson, W. S.; Harding, B. J.; Zhang, J.; Bennett, B. D.; et al. A comparison of folding techniques in the chemical synthesis of the epidermal growth factor-like domain in neu differentiation factor alpha/beta. *J. Pept. Res.* **2000**, *55*, 359−371.

(42) Shenkin, P. S.; McDonald, D. Q. Cluster Analysis of Molecular Conformations. *J. Comput. Chem.* **1994**, *15*, 899−916.

(43) Chen, W.; Shields, T. S.; Stork, P. J. S.; Cone, R. D. A Colorimetric Assay for Measuring Activation of Gs- and Gq-Coupled Signaling Pathways. *Anal. Biochem.* **1995**, *226*, 349−354.

(44) Haskell-Luevano, C.; Holder, J. R.; Monck, E. K.; Bauzo, R. M. Characterization of Melanocortin NDP-MSH Agonist Peptide Fragments at the Mouse Central and Peripheral Melanocortin Receptors. *J. Med. Chem.* **2001**, *44*, 2247−2252.

(45) Schild, H. O. pA, A New Scale for the Measurement of Drug Antagonism. *Br. J. Pharmacol.* **1947**, *2*, 189−206.

(46) Bowen, W. P.; Jerman, J. C. Nonlinear Regression Using Spreadsheets. *Trends Pharmacol. Sci.* **1995**, *16*, 413−417.